Mild fluctuations in wild ferroelastic domain switching

Yang Yang[1], Libo Zhang[1], Suzhi Li[1], Xiangdong Ding[1,*], Jun Sun[1], Jerome Weiss[2,*], and Ekhard K.H. Salje[1,3,*]

[1.] *State Key Laboratory for Mechanical Behaviour of Materials, Xi'an Jiaotong University, Xi'an 710049, China*

[2.] *IsTerre, CNRS/Université Grenoble Alpes, 38401, Grenoble, France*

[3.] *Department of Earth Sciences, University of Cambridge, Cambridge CB2 3EQ, UK*

[*] Authors to whom correspondence should be addressed:

dingxd@mail.xjtu.edu.cn (X.D.)
jerome.weiss@univ-grenoble-alpes.fr (J.W.)
ekhard@esc.cam.ac.uk (E.K.H.S.)

Abstract

We study the avalanche dynamics of shear-induced ferroelasticity by molecular dynamics simulations and statistical analysis. The dynamics of ferroelastic domain switching proceeds by avalanches which are power law distributed. These avalanches can therefore be classified as 'wild' with an energy exponent near 3. Wildness originates from the interaction between domain boundaries and defects, and jamming between domain boundaries. Concomitantly, 'mild' events also arise but their distributions do not follow power laws so that these 'mild energy releases' are not scale invariant and exhibit a characteristic energy. We identify several mild domain switching events, namely the motion of single kinks and highly non-linear relaxations of solitonic waves. The solitonic waves are reflected by domain boundaries, kinks, junctions, and free surfaces. Relaxations during domain switching have different characteristic energies from those created during creep. We observe the co-existence of mild and wild events depending on the external forces acting on the ferroelastic material.

I. Introduction

The deformation dynamics of ferroelastic materials attracts increasing research interests because many multi-ferroic materials are strongly ferroelastic, so that their high frequency behaviour is largely determined by their elastic behaviour. Ferroelectric or ferromagnetic switching, for example, is often dominated by domain wall movements which carry large strains. These movements also induce a ferroelastic hysteresis and carry with them the internal properties of the domain wall, such as a high conductivity, which is a key element in neuromorphic computation [1]. Experimentally, the dynamic behaviour is studied by the statistical analysis of avalanche 'jerk' signals e.g., measured from acoustic emission (AE) spectra during stress drops etc. Typically, power-law distributed jerks in space and time [2-4] are the signature of wild, scale-invariant avalanches, while Gaussian or exponentially distributed signals represent mild fluctuations and smooth plasticity [5]. Wild and mild plasticity are both common in metals. For example, in HCP materials [6], wild plasticity is dominant while in FCC metals with large system sizes, mild plastic jerks are more common [5]. Despite the urgency of this research, no systematic studies of the crossover between mild and wild avalanches in ferroelastics or multi-ferroics are known to the authors. Wild and mild jerks can coexist during plastic deformation in metals and alloys [7-11]. From this research we know that the wildness of dislocation-mediated plasticity is associated with the dislocation mean free path, which can be tuned by external and\or internal sizes [12-14]. As an example, the wildness of twinning-mediated plasticity in Fe nano-wires is associated with kink motions inside twin boundaries (TBs) and can be tuned by tailoring the twin boundary density [11].

The manipulation of TBs is also an effective way to achieve unique functional properties in materials because boundaries possess 'emerging' electronic transport [15], polarization [16-18], heat conduction [19] etc. which do not exist in the bulk. This is the fundamental idea of domain boundary engineering [20]. For example, the domain boundaries become superconducting in insulating WO_{3-x} [21]. Polar domain walls are observed in a non-polar bulk matrix in $CaTiO_3$ [22]. With the aid of TB motion, some functional properties such as superelasticity [23-27] are achieved at a nanoscale. When domain boundaries move, they carry these emerging properties with them so that the way they move determines how these properties evolve in space and time.

In this paper we focus on ferroelastic domain switching, which is induced by the movement of ferroelastic domain boundaries [28]. Due to their rich physics and potential importance, many studies focused on their deformation mechanisms [17,18,29-35]. It is widely accepted that the hysteretic ferroelastic domain switching is predominantly wild because of strong strain-induced correlations between domain boundary movements. The wildness can also stem from interactions between TBs and external defects such as vacancies, via the pinning-depinning mechanism [34,36-40], while small geometrical changes can fundamentally modify the behavior from abrupt (~wild) to smooth (~mild). Even in a system without defects, wall-wall interactions occur due to the formation of junctions between TBs [29,30,32]. Interactions related to stress fields by mobile kinks in TBs also induces wild avalanches [41]. On the other hand, mild fluctuations have been observed in many systems, such as in magnets [42], $BaTiO_3$ [43], and $SrTiO_3$ [44,45] etc., but have not yet been fully analyzed. It is the purpose of this paper to show that mild and wild fluctuations co-exist

during ferroelastic domain switching in ferroelastic materials. Not surprisingly, the much smaller, mild events are more difficult to detect experimentally. This justifies the present simulation study. We use molecular dynamics (MD) simulations to study shear-induced ferroelastic domain switching in an anharmonic Landau potential [46] and analyze the wild and mild dynamics statistically. Based on our analysis, we hope that an experimental analysis of mild fluctuations in shear-induced ferroelasticity from acoustic emission could be possible in the future.

II. Simulation method

We simulate the ferroelastic domain switching via a Landau-type potential, which is based on nonlinear elastic interactions (Landau springs) and harmonic springs. The potential energy U(r) contains three parts: the first-nearest atomic interactions $U_{NN} = 10(r - 1)^2$ $(0.8 < r < 1.2)$, the second-nearest atomic interactions $U_{NNN} = -10(r - \sqrt{2})^2 + 2000(r - \sqrt{2})^4$ $(1.207 < r < 1.621)$, and the third-nearest atomic interactions $U_{NNNN} = -(r - 2)^4$ $(1.8 < r < 2.2)$, where r is the interatomic distance. The equilibrium lattice constant a = 1 Å and atomic mass M = 10 amu. The spontaneous shear angle of 4° is taken to be the order parameter to indicate the domain structures. This potential has been widely used to simulate strain induced ferroelastic domain switching in our previous works [29,32,41].

A system including 40000 atoms (20 nm × 20 nm in dimension) with periodic boundary conditions was created to study the shear induced ferroelastic domain switching. The initial configuration contains a complex domain pattern with a high-density of TBs and junctions. The system was first relaxed in a canonical ensemble (NVT) for 1 ns. The external shear is applied to the simulation box at a constant strain rate of 10^7 s^{-1}. The maximum shear strain is 2%. Then the strain was kept and the structure was relaxed for 2 ns to simulate creep. The temperature was kept at 0.1 K using a Nosé-Hoover thermostat [47,48] during relaxation, shearing and creep to ensure an athermal structural evolution during domain switching [49,50]. All MD simulations were performed using the LAMMPS code [51]. The atomic patterns are displayed by the Open Visualization Tool (Ovito) software [52,53].

The jerky behavior of the ferroelastic deformation is quantified by the jerk strength J, which is the square of the first derivative of the system-size elastic energy stored in the system E_p as $J \sim (dE_p/dt)^2$, where dt is the timestep (5 fs) in our statistical analysis. This parameter is known as a slew rate in electrical engineering, plasma physics etc. [54]. Our previous work has showed that analyzing the dynamics from the jerk strength or from another signal like jerk energy reveals a very similar statistical behavior [11,55]. A power-law probability distribution function (PDF) of jerk strengths J corresponds to strong and collaborative movements of twin walls, indicating a 'wild' plasticity. In contrast, an exponential PDF indicates weak and random movements of defects, which is a signature of a 'mild' plasticity.

III. Results and discussion

A. Typical processes in shear induced ferroelastic domain switching

Fig. 1(a) shows the variation of the potential energy E_p (red) and the corresponding jerk spectrum (black) as a function of time t under shear at 0.1 K. The potential energy evolves by jerks. Structural evolution such as TBs movements occurs predominantly during large E_p drops, which induces larger jerks than during the prior increase of E_p. The maximum value of J during these large drops is two orders of magnitude higher than what is observed during the intervals between these large drops, when the potential energy mainly increases. The initial and final configurations are shown in Fig. 1(b) and 1(c). Starting from a complex twin pattern with a high-density of TBs and junctions (red lines in Fig. 1(b) and (c)), ferroelastic domain switching occurs at a very low critical stress. The structure evolution (from Fig. 1(b) to 1(c)) occurs during the energy-drop.

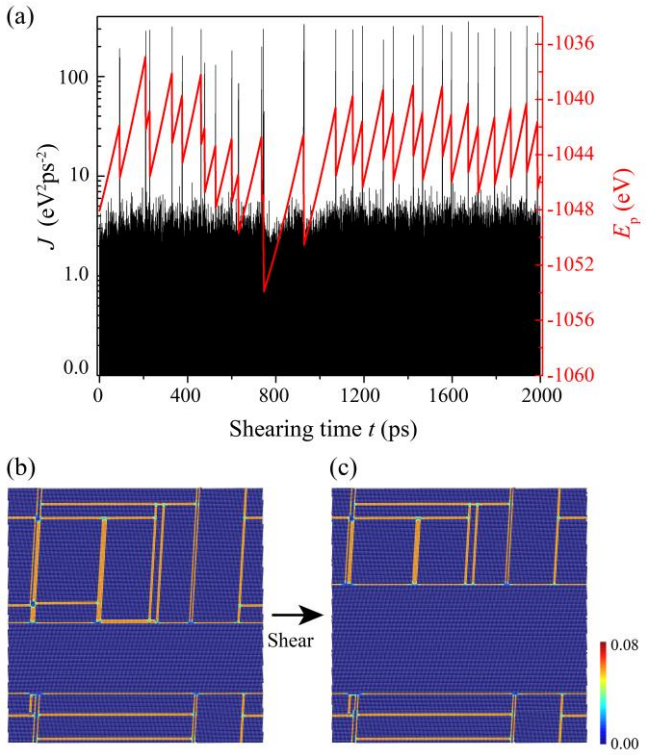

FIG. 1. Shear induced ferroelastic domain switching at 0.1 K. (a) Evolution of potential energy E_p (red) and corresponding jerk strength J (black) as function of shearing time (with linear shear rate). (b) Initial and (c) final configurations during shear induced ferroelastic domain switching. The atoms are colored by the centrosymmetry parameter [56].

We find three typical processes for the energy drops. Firstly, kinks nucleate and annihilate in TBs. Kinks usually form in high stress regions near junctions and surfaces. The nucleation and annihilation of kinks modify the TB morphology. The Fig. S1 and the Movie S1 in the Supplementary Material show how a kink sinks at a TB junction. Secondly, once a kink sinks at a junction, some solitary waves are activated, as shown in the Supplementary Material in Fig. S2 and Movie S2. These excitations are closely related to the local structural relaxation and can be considered as a secondary process during ferroelastic domain switching. The third process is the

propagation of a single kink. The motion of a kink ends up to be a domain boundary movement after a kink has traveled forward and backwards to the end of the TB. When a kink moves somewhere far from a junction, it behaves differently, which will be discussed below. The Fig. S3 and Movie S3 in the Supplementary Material show the motion of a single kink.

B. Avalanche analysis of the deformation process

All jerks during the shear deformation are now analysed (Fig. 2). Fig. 2(a) shows a small part of the jerk spectrum between 208 ps and 212 ps, and with measurable jerk strengths J between 10^{-2} to 10^{2} eV^2ps^{-2}. The probability distribution of all jerks in Fig. 1a shows a small strength range where the jerks are power law distributed ($J > 20$ eV^2ps^{-2}, see in Fig. 2(b)). Power law scaling breaks down below that value. The equivalent maximum likelihood (ML) evaluation [57] for all jerks in Fig. 1(c) shows a mixed statistical behavior with three different sources of events [58,59]. The first group corresponds to jerk strengths larger than 20 eV^2ps^{-2}. These large jerks are power-law distributed with an exponent of ~3 (Fig. 2(b)-(c)). These signals are the signature of avalanches representing the wild part of deformation process.

Two other regimes can be identified below this lower bound of the power law tail, around 20 eV^2ps^{-2}. In the second regime just below this lower bound, we find events with jerk strengths between ~3 and ~20 eV^2ps^{-2} corresponding to individual kink motions. These events occur after wild switching avalanches when the local strain deformations relax. During the relaxation the dominant movement is the nucleation and shift of kinks in domain walls. The corresponding J-values are exponentially distributed, $P(J) \sim \exp(-J/J_0)$. J_0 represents the characteristic jerk strength of this distribution, and $-J_0^{-1}$ is the parameter indicating its decreasing rate. With a characteristic strength J_0 of ca. 25 eV^2ps^{-2}, jerks between ~3 and ~20 eV^2ps^{-2} hence can be allocated to mild dynamics (Fig. S4).

After shear we observe that very weak movements occur with jerk strength below few eV^2ps^{-2}. These movements are related to lattice relaxations during switching. Their statistics is also ‘mild’ and related to the emission and scattering of solitary waves during lattice relaxations at times further away from the switching process. These dynamical excitations represent the third regime of strength values, below ~ 3 eV^2ps^{-2}, which also follows an exponential distribution with J_0 = ca. 3.1 eV^2ps^{-2}. In the Supplementary Materials we show movies of the three processes (Fig. S1-3 and Movie S1-3).

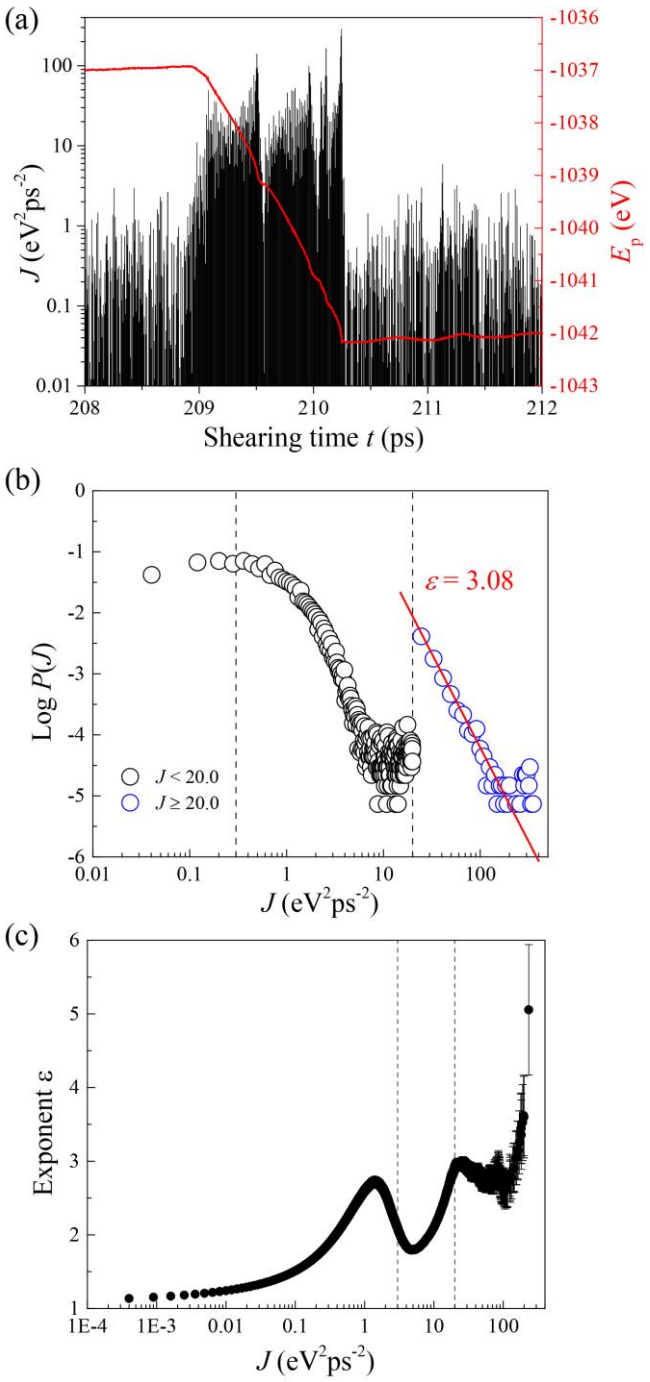

FIG. 2. A small segment of a jerk spectrum and corresponding potential energy (a) with three different motions intermingled. Jerks with strength larger than 20 eV^{2}ps^{-2} are power law distributed, hence can be classified as 'wild'. Smaller jerks are hidden in the spectra but are made visible by the analysis in (b) and (c). These signals are exponentially distributed and are classified as 'mild'. (b) Log-log plot of the PDF of jerk strength of all energy drops showing a limited power-law distribution with an exponent of ~3 and a long exponential tail at lower energies. The red line shows the power-law exponent $\varepsilon = 3$ for the high energy tail. For jerks at lower energies (< 20 eV^{2}ps^{-2}), we use an energy bin of 0.08 eV (black circles) and for jerks at higher energies we use an energy bin of 18.77 eV (blue circles). (c) Energy exponent calculated by the

by ML method showing a small plateau for $J > 20$ eV^{2}ps^{-2} over one decade and a large regime of statistical mixing. The *x* axis represents the lower cutoff for the jerk strengths such that only jerk strengths above this cutoff are considered for the ML analysis. The continuous increase of the exponent at small (below ~1 eV^{2}ps^{-2}) *J*-values indicate the exponential distribution of these data [59]. The dashed lines in (b) and (c) indicate the jerk strength boundaries of 3 eV^{2}ps^{-2} and 20 eV^{2}ps^{-2}.

Fig. 3 shows the statistical analysis of the strongest jerks only after separation of all other peaks. The PDF exhibits a power-law distribution, i.e. $P(J) \sim J^{-\varepsilon}$ with an exponent $\varepsilon = 3.08 \pm 0.14$, as shown in Fig. 3(a). The maximum likelihood (ML) analysis further validates the power law distribution (see Fig. 3) which represents wild avalanches. This data subset, corresponding to wild avalanches, is hence entirely determined by the ferroelastic switching of the sample. However, we also noticed that the power-law scaling is only observed over one decade. The lower bound is related to the physics, i.e. to the predominance of mild fluctuations below ~ 20 eV^{2}ps^{-2}. The upper bound is related to a finite-size effect. Fig. S5 shows this finite-size effect on the power-law distribution of jerk strengths. Here we mainly present the results obtained with a small simulation box (40000 atoms) as it is easier to correlate the mild fluctuations and the structure evolutions in such a small system.

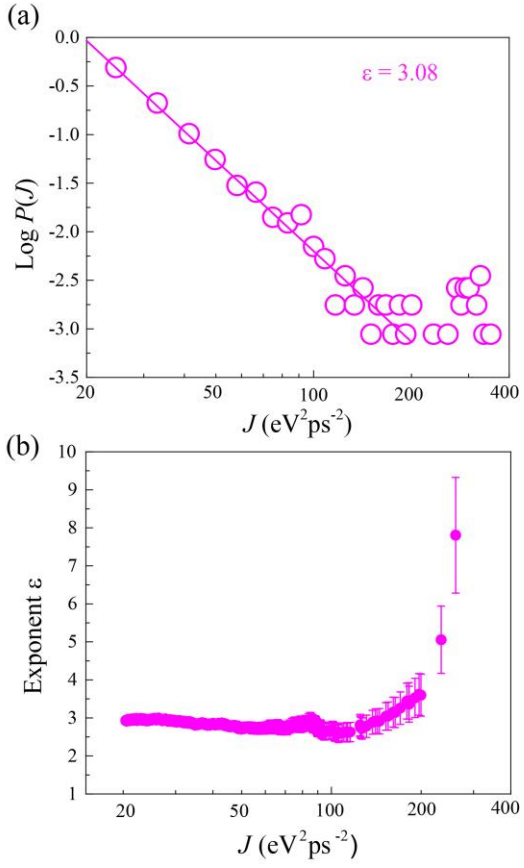

FIG. 3. Statistical analysis of jerks generated by kink nucleation and annihilation during ferroelastic domain switching at 0.1 K. (a) Log-log plot of the PDF of jerk strength showing a power-law distribution with an

exponent ε = 3.08±0.14 which characterizes wild dynamics. (b) Exponent analysis by the ML method shows a plateau over at least one order of magnitude.

We then separate the mild avalanches after the switching process (but not those in the creep regime when solitary waves are activated during and after switching (Fig. S2)). The phonon relaxations induce weak discontinuities of the potential energy. The jerks related to the phonon relaxation possess small characteristic jerk strength (< 3 ev^2ps^{-2}) and are exponentially distributed (Fig. 4(a)). This implies that the events are not scale invariant, instead they are exponentially distributed with a characteristic jerk strength J_0 = 3.1 eV^2ps^{-2}. The ML method shows high damping (Fig. 4(b)) and no plateau, as expected for exponential distributions [59]. These events correspond to a mild, overdamped dynamics.

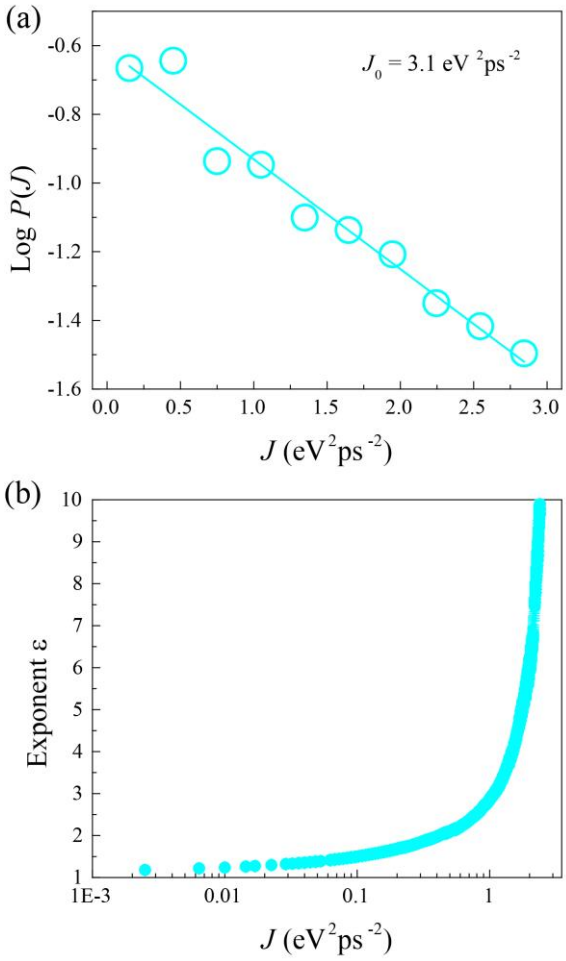

FIG. 4. Statistical analysis of jerks generated by anharmonic phonons during ferroelastic domain switching at 0.1 K. (a) Semi-log plot of the PDF of jerk strength showing an exponential distribution $P(J) \sim e^{-J/Jo}$ with a characteristic jerk strength J_0 = 3.1 ev^2ps^{-2}. (b) Exponent plot by the ML method showing no plateau [59].

Ferroelastic domain switching follows wild avalanche dynamics but also encompasses some mild processes. The mildness comes from single-kink movements and structural relaxations. The phonons are generated by wild events, e.g. kink nucleation or annihilation.

C. Mild relaxation during creep

Creep occurs when the external shear stain is kept constant [60,61] while the atoms relax in the simulation box. In our simulations, creep is maintained for 2 ns, which is too short to capture a full domain pattern evolution. However, 2 ns is long enough to observe phonon relaxations. The PDF of jerks in the creep regime follows an exponential distribution with J_0 = 1.6 eV^2ps^{-2} (supplementary Fig. S6). The ML evaluation shows results consistent with a mild dynamics.

J_0 represents the typical jerk strength or typical energy of phonon relaxations. The emission of solitary waves during creep is mainly caused by the stress field near junctions. Therefore, J_0 depends explicitly on the junction density [11]. Fig. 5(a) shows the PDFs of jerks in seven creep intervals with different initial structures, i.e. different junction densities. From sample #1 to #7, the junction density increases from 0 to ~0.1 nm^{-2} (see supplementary Fig. S7 see the domain patterns), and J_0 increases non-linearly with the junction density.

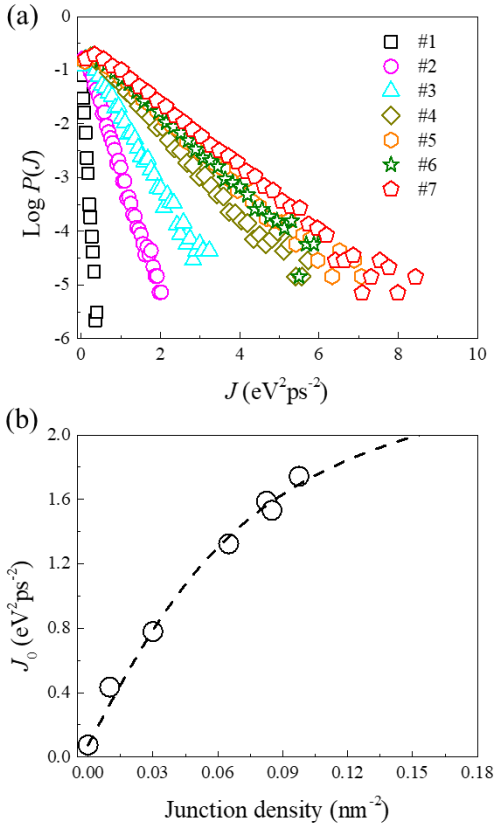

FIG. 5. Junction density dependent phonon relaxation in creep. (a) Semi-log plot of the PDFs of jerk strengths in samples with increasing junction density from sample #1 to #7 during creep. (b) J_0 evolution as a function of junction density during creep.

We empirically estimate the functional form by fitting the data in Fig. 5(b) with $J_0 = a\arctan(b\rho) + C$, where ρ is the junction density and C refers to J_0 at $\rho = 0$. With $a = 1.65$, we can estimate an upper limit of ~2.6 eV^2ps^{-2}, which is slightly smaller than the J_0 characteristic value for phonon relaxation during the actual domain switching process in Fig. 4a ($J_0 = 3.1$ eV^2ps^{-2}). The difference can be related to different activation mechanisms for the two scenarios. In contrast to events taking place during the creep process, events occuring during relaxation occur after wild switching.

D. Time correlations

In systems characterized by the coexistence of wild and mild fluctuations of energy dissipation, the wild jerks are intermittent, i.e. are correlated in time, while the mild fluctuations are uncorrelated [5]. To check this in our case, we proceeded as follows: we selected first the wild events, characterized by a jerk strength J larger than 20 eV^2ps^{-2} (see Figure 2(b)), and determined the waiting times t_w between these successive jerks during the shear simulations. The cumulative distribution of these waiting times is shown on Fig. 6(a).

This figure reveals a two-timescales structure. At the largest timescale, very large energy drops, readily apparent on Fig. 1(a), are pseudo-periodic, i.e. characterized by t_w values centered around 100 ps. In other words, these large drops are anti-clustered, characterized by a ratio between their standard deviation and their mean $\frac{\delta t_w}{\langle t_w \rangle} = 0.56 < 1$. This pseudo-periodicity likely results from finite-size effects: when large avalanches travel across the entire (small) system, this induces a system-size drop of potential energy, hence unloading the system. Under the applied constant shear-rate conditions, this generates a sort of repetitive "stick-slip" phenomenon associated to system-size large events.

When zooming inside such a single large drop (see e.g. Fig. 2(a)), the associated J-signal appears intermittent, with a ratio $\frac{\delta t_w}{\langle t_w \rangle} = 2.6 >> 1$ indicating a strong time-clustering of jerks, and a distribution of waiting times compatible with a power law, $P(t_w) \sim t_w^{-\varepsilon_w}$ with $\varepsilon_w = 1.9$ for t_w between ~0.3 and 10^{-2} ps. In other words, these large system-size energy drops take place through swarms of intermittent jerks. Such intermittency is consistent with the wild character of these jerks.

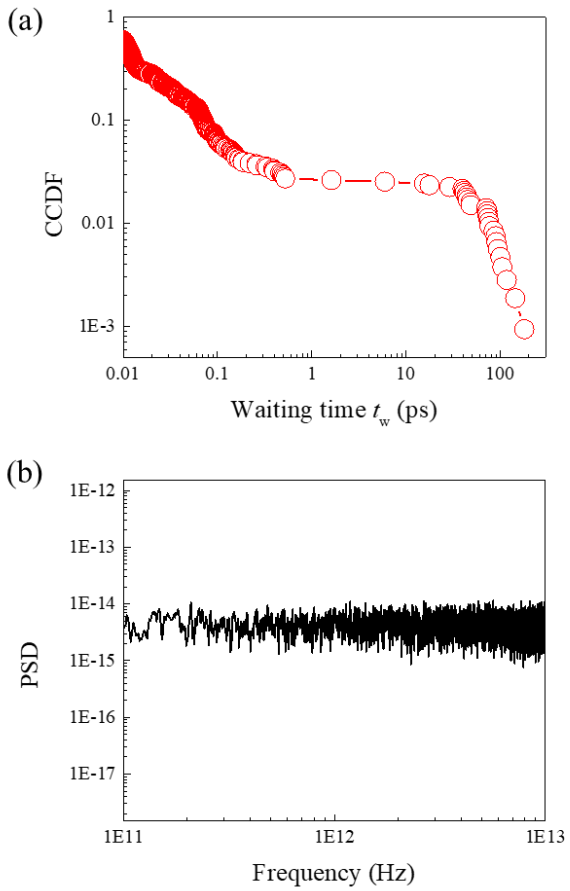

FIG. 6. Time correlations for wild and mild events during ferroelastic domain switching. (a) Complementary cumulative distribution function (CCDF) of waiting times between wild events. (b) Power spectral density (PSD) for jerks during creep.

On the reverse, the mild fluctuations of dE_p/dt observed in between these large drops, or during the creep simulation (section 3.3), are uncorrelated in time, as expected. Fig. 6(b) illustrates this for the creep simulation. The *J*-signal was first linearly detrended from its slow decay under such constant applied shear strain condition. This detrended signal exhibits a flat power spectral density (PSD) over the entire range of timescales explored, from 100 to 0.1 ps. This indicates an absence of time correlations, i.e. the mild signal has the characteristics of a white noise, as it was observed previously for mild fluctuations in crystalline dislocation dynamics [5]. We observed as well a flat PSD for the *J*-signals recorded during the intervals between large energy drops, in full agreement with their mild character.

To conclude on this section, the distinction made in the previous sections between wild and mild events during ferroelastic domain switching on the basis of the statistics of jerk strengths is mirrored in the time domain: mild fluctuations are uncorrelated, while intermittent wild jerks occur in swarms that eventually lead to system-size pseudo-periodic energy drops. This is consistent with what was previously reported for other systems [5,11].

IV. Conclusion

While avalanches during ferroic switching and martensitic transformations are confirmed to be power law distributed, we observe, in addition, mild dynamics inside the same jerk spectra. These mild events relate to local lattice relaxations which occur after the actual switching process or during creep experiments. Their physical origin is mainly due to kink movements inside domain walls for the relaxation after switching. Mild events during creep show even weaker effects by structural relaxations near intersections between domain walls. In detail, we find that

(a) wild and mild dynamics coexist in shear-induced ferroelastic domain switching. The wildness originates from sudden changes of domain patterns (generated by junctions and intersections of domain boundaries) or topological changes of domain boundary like kinks, nucleation, and annihilation. Mildness was found to dominate during single-kink movements and phonon-relaxations.

(b) Phonon relaxation during domain switching has a slightly higher activation strength J_0 than the emission of solitary waves during creep.

Acknowlegements

X.D. and J.S. are grateful to the NSFC (Nos. 51320105014 and 51621063) and the 111 Project (No. BP 2018008) for financial support. E.K.H.S. is grateful to EPSRC (No. EP/P024904/1) for support. S.L. acknowledges the support from NKRDPC (No. 2019YFA0307900). This project has received funding from the EU's Horizon 2020 Programme under the Marie Skłodowska-Curie Grant Agreement No. 861153.

References:

[1] E. K. H. Salje, APL Mater. **9**, 010903 (2021).
[2] J. Weiss and D. Marsan, Science **299**, 89 (2003).
[3] J. Weiss and M. C. Miguel, Mater. Sci. Eng., A **387**, 292 (2004).
[4] M. C. Miguel, A. Vespignani, S. Zapperi, J. Weiss, and J.-R. Grasso, Nature **410**, 667 (2001).
[5] J. Weiss, W. B. Rhouma, T. Richeton, S. Dechanel, F. Louchet, and L. Truskinovsky, Phys. Rev. Lett. **114**, 105504 (2015).
[6] J. Weiss, Philos. Trans. R. Soc. A **377**, 20180260 (2019).
[7] D. M. Dimiduk, C. Woodward, R. LeSar, and M. D. Uchic, Science **312**, 1188 (2006).
[8] S. Brinckmann, J.-Y. Kim, and J. R. Greer, Phys. Rev. Lett. **100**, 155502 (2008).
[9] P. Zhang, O. U. Salman, J. Zhang, G. Liu, J. Weiss, L. Truskinovsky, and J. Sun, Acta Mater. **128**, 351 (2017).
[10] Y. Yang, X. Ding, J. Sun, and E. K. H. Salje, Nanomaterials **11** (2021).
[11] Y. Yang, S. Li, X. Ding, J. Sun, J. Weiss, and E. K. Salje, Acta Materialia **195**, 50 (2020).
[12] S. Papanikolaou and G. Po, arXiv preprint arXiv:1906.01482 (2019).
[13] F. F. Csikor, C. Motz, D. Weygand, M. Zaiser, and S. Zapperi, Science **318**, 251 (2007).
[14] S. Papanikolaou, Y. Cui, and N. Ghoniem, Modell. Simul. Mater. Sci. Eng. **26**, 013001 (2018).
[15] C. Riek, D. V. Seletskiy, A. S. Moskalenko, J. F. Schmidt, P. Krauspe, S. Eckart, S. Eggert, G. Burkard, and A. Leitenstorfer, Science **350**, 420 (2015).
[16] E. K. H. Salje, S. Li, Z. Zhao, P. Gumbsch, and X. Ding, Appl. Phys. Lett. **106**, 212907 (2015).
[17] G. Lu, S. Li, X. Ding, and E. K. H. Salje, Appl. Phys. Lett. **114**, 202901 (2019).
[18] E. K. H. Salje, S. Li, M. Stengel, P. Gumbsch, and X. Ding, Phys. Rev. B **94**, 024114 (2016).
[19] S. Li, X. Ding, J. Ren, X. Moya, J. Li, J. Sun, and E. K. H. Salje, Sci. Rep. **4**, 6375 (2014).
[20] E. K. H. Salje and H. Zhang, Phase Transit. **82**, 452 (2009).
[21] A. Aird and E. K. H. Salje, J. Phys.: Condens. Matter **10**, L377 (1998).
[22] S. Van Aert, S. Turner, R. Delville, D. Schryvers, G. Van Tendeloo, and E. K. H. Salje, Adv. Mater. **24**, 523 (2012).
[23] Y. Yang, S. Li, X. Ding, and J. Sun, Comput. Mater. Sci., 110128 (2020).
[24] Y. Yang, S. Li, X. Ding, J. Sun, and E. K. H. Salje, Adv. Funct. Mater. **26**, 760 (2016).
[25] S. Li, E. K. H. Salje, J. Sun, and X. Ding, Acta Mater. **125**, 296 (2017).
[26] K. Otsuka, H. Sakamoto, and K. Shimizu, Scripta Metall. **11**, 41 (1977).
[27] S. Li, X. Ding, J. Li, X. Ren, J. Sun, and E. Ma, Nano Lett. **10**, 1774 (2010).
[28] E. Salje, Ferroelectrics **104**, 111 (1990).
[29] X. Ding, T. Lookman, E. K. H. Salje, and A. Saxena, JOM **65**, 401 (2013).
[30] X. Ding, T. Lookman, Z. Zhao, A. Saxena, J. Sun, and E. K. H. Salje, Phys. Rev. B **87**, 094109 (2013).
[31] A. S. Everhardt, S. Damerio, J. A. Zorn, S. Zhou, N. Domingo, G. Catalan, E. K. H. Salje, L.-Q. Chen, and B. Noheda, Phys. Rev. Lett. **123**, 087603 (2019).
[32] X. He, S. Li, X. Ding, J. Sun, S. M. Selbach, and E. K. H. Salje, Acta Mater. **178**, 26 (2019).
[33] G. Lu, S. Li, X. Ding, J. Sun, and E. K. H. Salje, Phys. Rev. Mater. **3**, 114405 (2019).
[34] G. F. Nataf and E. K. H. Salje, Ferroelectrics **569**, 82 (2020).
[35] Z. Zhao, X. Ding, T. Lookman, J. Sun, and E. K. H. Salje, Adv. Mater. **25**, 3244 (2013).
[36] L. X. Hayden, A. Raju, and J. P. Sethna, Physical Review Research **1**, 033060 (2019).
[37] A. Dobrinevski, P. Le Doussal, and K. J. Wiese, EPL (Europhysics Letters) **108**, 66002 (2015).
[38] H.-S. Lee, K.-S. Ryu, K.-R. Jeon, S. S. P. Parkin, and S.-C. Shin, Phys. Rev. B **83**, 060410 (2011).
[39] P. Le Doussal and K. J. Wiese, Phys. Rev. E **79**, 051105 (2009).
[40] P. Le Doussal, M. C. Marchetti, and K. J. Wiese, Phys. Rev. B **78**, 224201 (2008).
[41] L. Zhang, S. Li, X. Ding, J. Sun, and E. K. H. Salje, Appl. Phys. Lett. **116**, 102902 (2020).
[42] S. K. Nandi, G. Biroli, and G. Tarjus, Phys. Rev. Lett. **116**, 145701 (2016).

[43] B. Casals, G. F. Nataf, D. Pesquera, and E. K. H. Salje, APL Mater. **8**, 011105 (2020).
[44] B. Casals, G. F. Nataf, and E. K. H. Salje, Nat. Commun. **12**, 1 (2021).
[45] B. Casals, S. van Dijken, G. Herranz, and E. K. H. Salje, Physical Review Research **1**, 032025 (2019).
[46] E. K. H. Salje, X. Ding, Z. Zhao, T. Lookman, and A. Saxena, Phys. Rev. B **83**, 104109 (2011).
[47] S. Nose, J. Chem. Phys. **81**, 511 (1984).
[48] W. G. Hoover, Phys. Rev. A **31**, 1695 (1985).
[49] Z. Zhao, X. Ding, J. Sun, and E. K. H. Salje, J. Phys.: Condens. Matter **26**, 142201 (2014).
[50] S. I. Rao, D. M. Dimiduk, T. A. Parthasarathy, M. D. Uchic, M. Tang, and C. Woodward, Acta Mater. **56**, 3245 (2008).
[51] S. Plimpton, J. Comput. Phys. **117**, 1 (1995).
[52] A. Stukowski, Modell. Simul. Mater. Sci. Eng. **18**, 015012 (2009).
[53] A. Stukowski and K. Albe, Modell. Simul. Mater. Sci. Eng. **18**, 025016 (2010).
[54] F. Liu, G. Huang, and B. Ganguly, Plasma Sources Sci. Technol. **19**, 045017 (2010).
[55] X. He, X. Ding, J. Sun, and E. K. H. Salje, Appl. Phys. Lett. **108**, 072904 (2016).
[56] C. L. Kelchner, S. J. Plimpton, and J. C. Hamilton, Phys. Rev. B **58**, 11085 (1998).
[57] J. Baró and E. Vives, Phys. Rev. E **85**, 066121 (2012).
[58] E. K. H. Salje, H. Liu, Y. Xiao, L. Jin, A. Planes, E. Vives, K. Xie, and X. Jiang, Phys. Rev. E **99**, 023002 (2019).
[59] E. K. H. Salje, A. Planes, and E. Vives, Phys. Rev. E **96**, 042122 (2017).
[60] E. K. H. Salje, H. Liu, L. Jin, D. Jiang, Y. Xiao, and X. Jiang, Appl. Phys. Lett. **112**, 054101 (2018).
[61] J. Baró, K. A. Dahmen, J. Davidsen, A. Planes, P. O. Castillo, G. F. Nataf, E. K. H. Salje, and E. Vives, Phys. Rev. Lett. **120**, 245501 (2018).